Changes in Pluto's atmosphere revealed by occultations (20 july and 21 august 2002)

F. Roques[1], B. Sicardy[1,2], T. Widemann[1], E. Lellouch[1], C. Veillet[3], J.-C. Cuillandre[3], F. Colas[4], W. Beisker[5], M. Kretlow[5], E. Gendron[1], J. Lecacheux[1], C. Birnbaum[7], A. Fienga[4], C. Leyrat[1], A. Maury[8], E. Raynaud[1], S. Renner[1], M. Schultheis[9], K. Brooks[10], A. Delsanti[1], O. R. Hainaut[10], R. Gilmozzi[10], C. Lidman[10], J. Spyromilio[10]

[1]*Observatoire de Paris, LESIA, 92195 Meudon, France,*
[2]*Université Pierre et Marie Curie, 4 Place Jussieu, 75005 Paris, France,*
[3]*Canada-France-Hawaii Telescope, Waimea, Hawaii 96743, USA,*
[4]*Observatoire de Paris, IMCCE, 75014 Paris, France,*
[5]*International Occultation Timing Association, European Section, Germany,*
[7]*Cité des Sciences et de l'Industrie, 75930 Paris, France,*
[8]*Gene Shoemaker Observatory, San Pedro de Atacama, Chile,*
[9]*Institut d'Astrophysique de Paris, 75014 Paris, France,*
[10]*European Southern Observatory, Alonso de Córdova 3107, Casilla 19001, Santiago 19 Chile*

Abstract

Stellar occultations observed in july and august 2002 reveal drastic changes undergone by Pluto's atmosphere since the last occultation in 1988. These changes are best explained by a two-fold pressure increase revealing the effect of seasonal changes on Pluto. Thus, although the distance of Pluto to the Sun increased by 3%, its South Pole went from continuous darkness to continuous illumination, probably triggering a sublimation of fresh nitrogen ice. This provides insights into surface-atmosphere interactions and temporal variability on distant icy bodies of the solar system, and may help for the preparation of a space mission to Pluto.

1 Introduction

Pluto's tenuous nitrogen atmosphere was first detected by stellar occultation in 1985 (ref. 1) and more extensively studied during a second event in June 1988 (refs. 2–6). Owing to the small angular diameter of Pluto on the sky (0.12 arcsec), these events are rare and only in 2002, on the 20th of July and 21st of August, was Pluto's atmosphere observed again using stellar occultations. Consequently, Pluto's atmosphere (not yet visited by a spacecraft) remains poorly known. This article is an extention of a paper published in Nature (ref. 7).

2 Observations

The stars occulted by Pluto on 20 July 2002 and 21 August 2002 are referred to as P126 and P131.1, respectively, in the candidate list of S.W. McDonald and J.L. Elliot[8,9]. We organized a campaign for the P126 event, using fixed and portable telescopes in Argentina, Brazil, Chile, Ecuador, Peru and Venezuela, while the P131.1 occultation was observed at the Canada-France-Hawaii Telescope (CFHT) in Hawaii.

2.1 The P126 event

Due to weather conditions and astrometric uncertainty prior to the event, we obtained only one positive detection of the P126 event in northern Chile near Arica, using a portable telescope and a broad band CCD camera peaking in sensitivity near 0.6 μm (Fig. 1a).

The imager was oriented with its lines parallel to the celestial Equator, and a scan of the stellar flux was performed at a rate of 100 milliseconds per column while the telescope was tracking. This scan finally provides the occultation lightcurve (stellar flux *vs.* UT time). Time benchmarks were generated manually by blocking at given intervals (provided by a GPS) the aperture of the telescope, yielding an absolute timing accuracy of about $\pm$ 0.3 sec. In order to monitor and correct for possible sky transparency variations, we divided the lightcurve (stellar flux *vs.* UT time) by the flux of an unocculted reference star 87 arcsec North of P126. yielding the normalized lightcurve of Fig. 1a. Since P126 is a multiple star, with the brightest components P126A (the occulted star) and P126B separated by only 2.25 arcsec, the lightcurve actually contains the combined signals of P126A, P126B, Pluto and its satellite Charon (adaptive optics images made at VLT show a third star in the system, P126C, but its flux is small enough that it can be neglected). Images taken at Pic du Midi Observatory with the same equipment broad band camera prior to the observation show that P126A is 1.9$\pm$0.1 times brighter than P126B, and that the P126A flux represents 46%$\pm$1% of the total unocculted flux, eventually providing the zero stellar flux baseline shown in Fig. 1a.

2.2 The P131.1 event

The P131.1 event was observed with high signal to noise ratio in a narrow I band filter at 0.83$\pm$0.1μm using the CFHT (Figs. 1bc). The exposure time was 1 sec, with an acquisition cycle of 1.583 sec, and an absolute time accuracy of 0.3 sec. The combined signal from Pluto, Charon, and the occulted star, which was divided by that of a reference star, located at 20 arcsec West of P131.1. yielding the normalized curve of Fig. 1b. Calibrations, made the night after the event, show that P131.1 contributes to 21%±0.5% of the total unocculted flux, yielding the zero stellar flux baseline oulined in (Fig. 1b).

3 Difference with 1988

Our lightcurves are significantly different from those obtained in 1988. In particular, the Kuiper Airborne Observatory (KAO) data exhibited an abrupt change of slope in their lower part, which is absent in our data, see Figs. 1ab. This sudden drop was interpreted as due to either absorbing hazes, or to a sharp inversion layer in the lowest 20-50 km above Pluto's surface, connecting the isothermal upper atmosphere at $T \approx$ 95-110 K to the ground temperature at $T \approx$ 40-60 K. Thus, our observations show that drastic changes in temperature or pressure, or both, occurred in Pluto's lower atmosphere during the 14 years interval separating 1988 and 2002. However, no obvious differences in the shape of the upper part of the lightcurves are visible, suggesting that the thermal structure of Pluto's upper atmosphere has remained largely unchanged since 1988.

4 Retrieval of temperature and pressure profiles

Occultation lightcurves can in principle be inverted to obtain the atmospheric number density n, temperature T, and pressure p as a function of distance r to the planet center. This inversion requires, for each time step, the distance ρ of the observer to the center of Pluto's shadow projected on Earth. This distance was retrieved with high accuracy (~ 15 km) for the 1988 event because several occultation chords were available. This, combined with KAO data error bars, provides the 1988 pressure profile shown in Fig. 2c (refs. 4,6). Conversely, with one chord at hand for the P126 and P131.1 events, the typical uncertainty on ρ is 250 km for both events, (or 12 milliarcsecs projected at Pluto's distance), as derived from astrometric measurements available for each star and Pluto (see $e.g.$ http://occult.mit.edu). From these measurements, the expected closest approaches $\rho_{\rm min}$ of the Arica and Hawaii stations to the shadow center were $\rho_{\rm min} = 975 \pm 250$ km and $\rho_{\rm min} = 610 \pm 250$ km, respectively, showing that the P131.1 event was more central than the P126 one.

We will use these nominal values hereafter, while more accurate values will be available when all the lightcurves obtained during these events are available for a consistent comparison.

Only the higher quality P131.1 lightcurve has been inverted, and to within the astrometric uncertainties described above, all our inversions show that the temperature or pressure profiles (or both) have drastically changed since 1988. In particular, taking the nominal astrometric solution corresponding to $\rho_{\rm min} = 610$ km, we obtain essentially the same temperature profile $T(r)$ as in 1988, including a strong inversion layer below $r = 1215$ km, but with a systematic and significant increase of pressure at all radii (see Fig. 2c). This pressure increase reaches a factor of 2.1 at $r = 1215$ km, where $p = 5.0\pm0.6$ μbars in 2002, while $p = 2.33\pm0.24$ μbars in 1988 (ref. 6).

5 Limb to limb asymmetry

Fig. 1c shows that the bottom of the P131.1 lightcurve is generally flat for about 200 sec, with a small but significant decrease of signal over this time interval. Taking again the nominal astrometric solution corresponding to $\rho_{\rm min} = 610$ km, we find that during this 200 sec interval the image of P131.1 scanned Pluto's limb at a constant radius of 1205 km, with latitudes ranging from 61°S (ingress) to 8°S (egress) (Fig. 3). This steady decrease of signal could conceivably be due to the presence of morning hazes above the egress point. Perhaps more probably, it indicates an egress temperature about 10 K smaller than the ingress temperature at $r = 1205$ km. The P131.1 star ingress probed the South Pole region now constantly in sunlight, while the egress probed the morning limb of the equatorial region, which emerged after 3.2 days in darkness. (Note that we adopt the International Astronomical Union convention, in which Pluto's South Pole is currently tilted toward the Earth). Taking a thermal inertia $\Upsilon = 15$ J m^{-2} s$^{-1/2}$ K^{-1}, derived from Pluto's thermal lightcurve[10], and using a subsolar latitude of 29.7°S at Pluto in August 2002, we estimate that the dawn equatorial ground temperature is $\sim 25\%$ lower, *i.e.* 12-15 K cooler, than the polar temperature for a uniform surface albedo. This temperature difference can however be reduced if the terrains covering the South Pole are brighter than those at the Equator. In effect, according to a recent surface model[11], Pluto's South Pole is covered by methane-rich areas while the Equator is predominanly covered by darker tholins. For this case, we estimate a ground polar temperature of $\sim$ 53 K and a dawn equatorial temperature of 45 K. These numbers compare well with the difference between the immersion and emersion temperatures near $r=$ 1205 km, suggesting that the lower 10-40 km (0.25-1 scale height) of the atmosphere are affected by surface boundary layer effects.

6 Pluto's upper atmosphere

Conversely, our observations do not discern a significant temperature difference between egress and ingress (and also with 1988) in the isothermal region above $r=$ 1220 km. This can be understood in the methane-thermostat model of Yelle and Lunine[12] which demonstrates that the upper atmosphere temperature is robustly controlled at $\sim$100 K by the radiative properties of atmospheric CH_4, almost independently of its abundance. Accounting for the diurnally-averaged insolations at the South Pole and the Equator, we find that the upper atmospheric temperatures at ingress and egress should only differ by 3 K at radiative equilibrium, well within the uncertainties of our measurements. Note also that dynamical effects would further reduce this difference.

7 Spikes

The P131.1 lightcurve exhibits spikes (Fig. 1c) which correspond to local temperature gradients of up to $dT/dr \approx \pm$ 0.05 K km^{-1} over vertical scales of 5-15 km in the retrieved temperature profiles (Fig. 2b), yielding temperature fluctuations of $\Delta T \approx \pm$ 0.5-0.8 K over these scales. The spikes are quite more conspicuous than in 1988 (refs. 4,6), and reveal a dynamical activity in Pluto's atmosphere. Its origin could be gravity waves launched by convection in a putative lower troposphere, and/or turbulence triggered by shears driven by strong winds between Pluto's lit and dark hemispheres[10]. The observed values of $|dT/dr|$ remain well below the adiabatic temperature lapse rate Γ (Fig. 2b), indicating that either convective instability is not reached, or that stronger local gradients exist but are smoothed out over the $\approx$ 500 km that a stellar ray travels in the atmosphere before being significantly refracted towards the Earth.

8 Discussion

We have tested the robustness of our results *vs.* changes in the P131.1 astrometric solution. We find that varying $\rho_{\min}$, everything equal besides, mainly displaces vertically the temperature profile $T(r)$, while multiplying the pressure at all levels by a roughly constant factor with respect to the nominal solution with $\rho_{\min} = 610$ km. In particular, a solution that leaves the pressure unchanged at all levels (to within 10%) since 1988 can be found with $\rho_{\min} = 550$ km. However, the whole temperature profile $T(r)$, including the inversion layer, would then be shifted downward by about 30 km. Such a large variation of Pluto's thermal structure in the lower atmosphere since 1988 seems unlikely. The inversion layer is best physically explained through the absorption by atmospheric methane, and its existence does not sensitively depend on the CH_4 abundance (although the precise value of the temperature gradient does[13]). Moving the inversion layer downward by 30 km from its $r=$ 1200-1220 km nominal level would imply a dramatic shrinking of the 40 km deep troposphere advocated for by Stansberry *et al.*[14] on the basis of the 1988 occultation. Such a troposphere would presumably be maintained by convection, perhaps driven by the large temperature gradients across Pluto's surface[10]. It should be fairly stable over a 14 year timescale, and it is supported by the presence of spikes in the CFHT lightcurve as discussed above. In contrast, a two-fold increase in pressure in 14 years since 1988 is not at odds with expectations of nitrogen cycle models[15,16], despite Pluto's increasing heliocentric distance. In the best fitting model of Hansen and Paige[15] the pressure increases by a factor of about 10 over 1980-2015, and by a factor of about 2 over 1990-2000. Best fitting models[15], in which N_2 frost distribution and associated atmospheric pressure are calculated as a function of season, do predict an increase of pressure by a factor of about ten over 1980-2015, and by a factor of about two over 1990-2000. This period follows the equinox on Pluto in 1987 which leads to the current sublimation of the South Polar Cap going into sunlight. Thus, although the seasonal models are only partly successful in reproducing the observed albedo patterns, particularly the currently large Northern Polar Cap and relative darkness of the South Polar regions, they must adequately capture the physics of hemispherical volatile exchange. □

References

1. Brosch, N. The 1985 stellar occultation by Pluto. *Mon. Not. R. Astron. Soc.* **276**, 571–578 (1995).
2. Hubbard, W.B., Hunten, D.M., Dieters, S.W., Hill, K.M. & Watson, R.D. Occultation evidence for an atmosphere on Pluto. *Nature* **336**, 452–454 (1988).
3. Elliot, J.L. *et al.* Pluto's atmosphere. *Icarus* **77**, 148–170 (1989).
4. Elliot, J.L. & Young, L.A. Analysis of stellar occultation data for planetary atmospheres. I. Model fitting, with application to Pluto. *Astron. J.* **103**, 991–1015 (1992).
5. Millis, R. L. *et al.* Pluto's radius and atmosphere - Results from the entire 9 June 1988 occultation data set. *Icarus* **105**, 282–297 (1993).
6. Yelle, R.V. & Elliot J.L. Atmospheric structure and composition: Pluto and Charon. In *Pluto and Charon* (Ed Stern S.A. & D.J. Tholen) 347–390 (University of Arizona Press, 1997).
7. Sicardy, B. *et al.* Drastic changes in Pluto's atmosphere revealed by stellar occultations. *Nature* **in press** (2003).
8. McDonald, S.W. & Elliot, J.L. Pluto-Charon stellar occultation candidates: 2000-2009. *Astron. J.* **119**, 1999–2007 (2000).
9. McDonald, S.W. & Elliot, J.L. Erratum: "Pluto-Charon stellar occultation candidates: 2000-2009". *Astron. J.* **120**, 1599–1602 (2000).
10. Lellouch, E. *et al.* Pluto's Non-isothermal Surface. *Icarus* **147**, 220–250 (2000).
11. Grundy W.M. & Buie M.W. Distribution and evolution of CH_4, N_2 and CO ices on Pluto's surface: 1995 to 1998. *Icarus* **153**, 248–263 (2001).
12. Yelle, R.V. & Lunine, J.I. Evidence for a molecule heavier than methane in the atmosphere of Pluto. *Nature* **339**, 288–290 (1989).
13. Strobel, D.F., Zhu, X., Summers, M.E. & Stevens, M.H. On the vertical thermal structure of Pluto's atmosphere. *Icarus* **120**, 266–289 (1996).

14. Stansberry, J.A., Lunine, J.I., Hubbard, W.B., Yelle, R.V. & Hunten, D.M. Mirages and the nature of Pluto's atmosphere. *Icarus* **111**, 503–513. (1994).

15. Hansen, C.J. & Paige, D.A. Seasonal Nitrogen Cycles on Pluto *Icarus* **120**, 247–265 (1996).

16. Spencer, J.R. *et al.* Volatile transport, seasonal cycles and atmospheric dynamics on Pluto. In *Pluto and Charon* (Eds Stern S.A. & D.J. Tholen) 435–475 (University of Arizona Press, 1997).

17. Sicardy, B. *et al.* The structure of Titan's stratosphere from the 28 Sgr occultation. *Icarus* **142**, 357–390 (1999).

18. Null, G.W. & Owen, Jr., W.M. Charon/Pluto mass ratio obtained with *HST* CCD observations in 1991 and 1993. *Astron. J.* **111**, 1368–3181 (1996).

Acknowledgements. We thank the Conseil Scientifique of Paris Observatory and the Programme National de Planétologie for supporting part of the observations of the P126 event in South America. We are grateful to C. Angeli, A. Bruch and D. Lazzaro who made the observational campaign possible in Brazil.

Figure captions

Figure 1: Dimming of the occulted stars P126 (20 July 2002) and P131.1 (21 August 2002) during their occultations by Pluto's atmosphere. a: the P126 lightcurve *vs.* time, binned in 2 sec time intervals in order to reduce the scintillation noise. This curv was obtained from northern Chile (long= 69°45'51.5"W, lat= 18°26'53.8"S, alt= 2500 m) with a 30-cm Schmidt-Cassegrain portable telescope and a Kodak KAF-401E CCD camera without filter, sensitive between 0.4 and 0.9 μm, with a peak near 0.6 μm. The horizontal length of the shaded rectangle represents a duration of 2 mn, centered at 01:44:03 UT. The total unocculted flux (P126 + Pluto + Charon) is normalized to unity (label "1") outside the occultation. The expected level corresponding to the complete extinction of the star (label "0") is indicated by the position of the shaded rectangle, whose vertical extension represents the uncertainty of photometric calibration. b: The P131.1 lightcurve, obtained at the Canada-France-Hawaii 3.55-m f/8 telescope (CFHT) equipped with a MIT/LL CCID20 in the I band (0.83±0.1μm) with a exposure time of 1 sec and cycle time of 1.583 sec. The length of the shaded rectangle now corresponds to a duration of 5 mn, centered at 06:50:35 UT. Graphs a and b are plotted with the same vertical scale from "0" to "1". The two horizontal scales are such that equal horizontal lengths represent equal distances travelled by Pluto in the plane of the sky. Both lightcurves have absolute timing accuracy of about 0.3 sec. The solid curve superimposed to each diagram is a is a smoothed version of the data obtained from Kuiper Airborne Observatory (KAO) during the 9 June 1988 Pluto occultation[3−6]. c: a vertically stretched version of b, enhancing the spikes ("S") and the steady decrease of signal in the bottom part of the lightcurve.

Figure 2: Temperature and pressure profiles of Pluto's atmosphere derived from the inversion of the P131.1 lightcurve. This inversion[17] assumes a spherically symmetric and transparent atmosphere. It first provides the atmospheric refractivity profile, then the density profile for a given gas composition, and finally the temperature profile, assuming an ideal gas in hydrostatic equilibrium. For Pluto a pure molecular nitrogen[6] atmosphere is assumed, and the curvature of Pluto's limb is taken into account as well as the variation of the acceleration of gravity g with radius, assuming a mass of 1.31×10^{22} kg for Pluto[18]. a: Pluto's atmospheric temperature profiles $T(r)$ at immersion (thick curve) and emersion (thin curve). The radius is the distance to the planet center, for the nominal astrometric solution discussed in the text. b: the corresponding temperature gradient profiles dT/dr. The dash-dotted line provides the adiabatic lapse rate profile $\Gamma = -g/c_p$ at the left of which the atmosphere would become convectively unstable, where $c_p = 1.04 \times 10^3$ J K^{-1} kg^{-3} is the specific heat at constant pressure for N_2. c: the corresponding pressure profiles. The dash-dotted line is the pressure profile derived from the KAO lightcurve of 9 June 1988 (ref. 6), with the associated error domain (Ibid.) shown as the shaded region. The immersion and emersion profiles derived from the CFHT lightcurve of 2002 are the nearly coincident thick and thin solid lines, respectively. The error domain for the 2002 profiles only takes into account the photometric uncertainties in the levels "0" and "1" shown in Fig. 1b. The effects of the astrometric uncertainty are discussed in the text.

Figure 3: Dotted line: the expected stellar paths of P126 (20 July 2002) and P131.1 (21 August 2002) with respect to Pluto. Solid curves: the actual trajectory followed by the stellar images, due to Pluto's atmospheric refraction. The radius of the planet plotted here (1150 km) is the preferred value derived from the mutual events with Charon in the late 1980's. The thin dark layer near Pluto's limb is where the stellar flux was attenuated by more than 50%, while the outer lighter region corresponds to a star dimming of 10%.

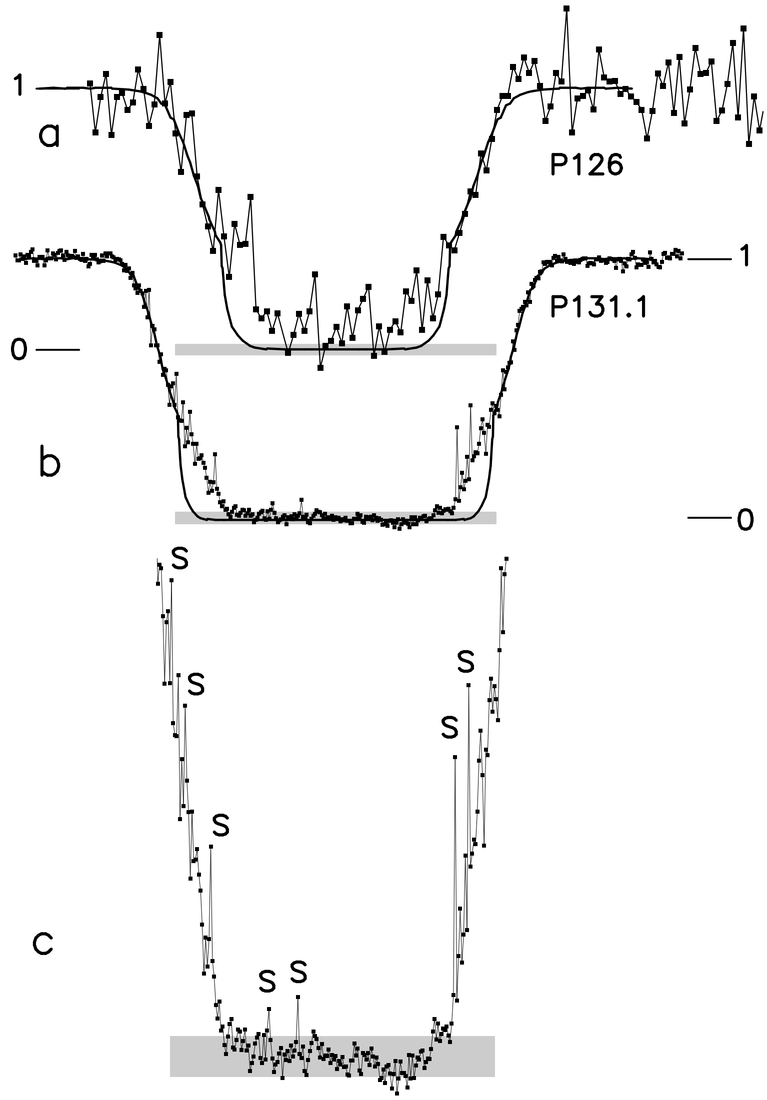

Figure 1

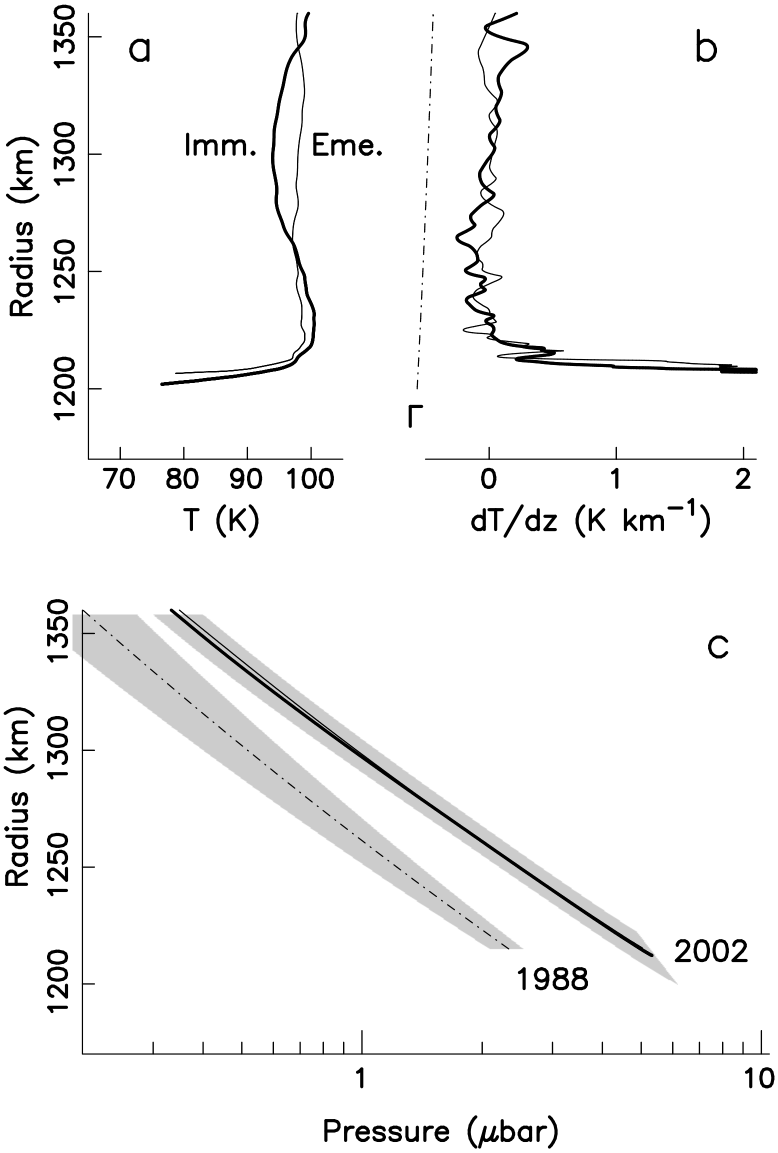
a
b
c
Imm.
Eme.
Γ
Radius (km)
1350
1300
1250
1200
70
80
90
100
T (K)
0
1
2
dT/dz (K km^{-1})
1988
2002
1
10
Pressure (μbar)

Figure 2

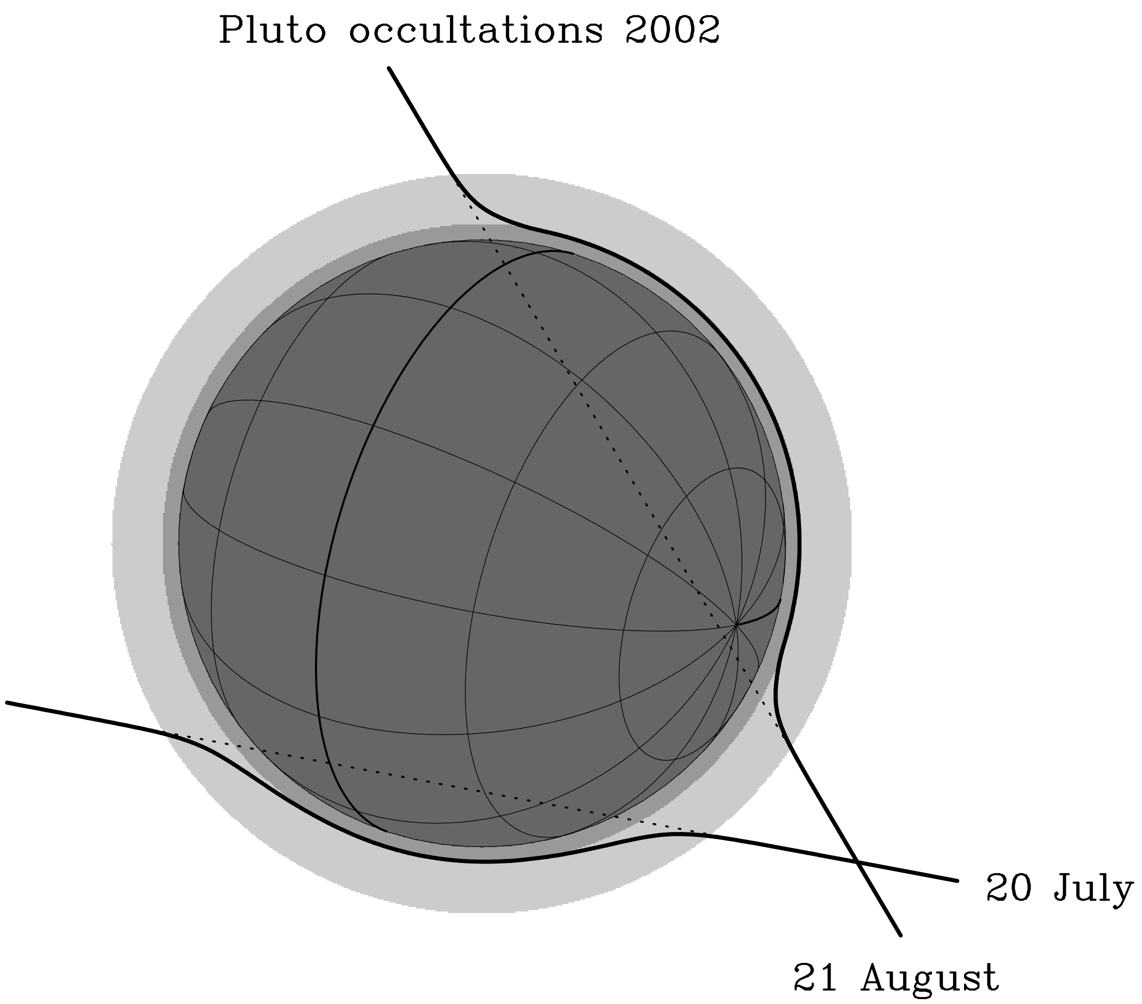

Figure 3